Available online at www.sciencedirect.com

European Journal of Mechanics A/Solids 23 (2004) 993–1005

Dynamic behavior of unequal parallel permeable interface multi-cracks in a piezoelectric layer bonded to two piezoelectric materials half planes

Jian-Liang Sun *, Zhen-Gong Zhou, Biao Wang

Center for Composite Materials and Electro-Optics Technology Center, Harbin Institute of Technology, P.O. Box 1247, Harbin, 150001, PR China

Received 20 January 2004; accepted 14 May 2004

Available online 29 July 2004

Abstract

This study is concerned with the treatment of the dynamic behavior of interacting cracks in a piezoelectric layer bonded to two dissimilar piezoelectric half planes subjected to harmonic anti-plane shear waves. The permeable electric boundary condition is considered. By use of the Fourier transform technique, the problem can be solved with the help of two pairs of dual integral equations in which the unknown variables are the jumps of the displacements across the crack surfaces. To solve the dual integral equations, the jumps of the displacements across the crack surfaces are expanded in two series of Jacobi polynomials. The electromechanical behavior of two pairs of unequal parallel cracks was determined. Numerical examples are provided to show the effects of the geometry of the cracks, the frequency of the incident waves and materials properties upon the dynamic stress intensity factors (DSIFs) and the electric displacement intensity factors.

Keywords: Interface cracks; Dynamic stress Intensity factors; Schmidt method

1. Introduction

Due to the inherent direct and converse piezoelectric effects between mechanical deformation and electric field, piezoelectric materials have been widely used in transducers and sensors. Among the piezoelectric materials, piezoelectric ceramics are widely used due to their high piezoelectric performance. However, piezoelectric ceramics in mechanical behavior are brittle and susceptible to cracking. Therefore, it's necessary to analyze theoretically and describe accurately quantitatively the damage and fracture processes taking place in piezoelectric materials.

Piezoelectric materials are mostly being used or considered for use in situations where dynamic loading is involved. Therefore, it's more important to study dynamic mechanics of these materials. Chen and Yu (1998) investigated the anti-plane vibration of infinite cracked piezoelectric medium with a single crack under impermeable electric boundary condition. Narita and Shindo (1998) solved the problem of a line crack subjected to horizontally polarized shear waves in an arbitrary direction with the help of the dynamic theory of anti-plane piezoelectricity. Meguid and Wang (1998) studied the dynamic interaction be-

* Corresponding author. Tel.: +86-451-8641-2613.
E-mail address: jlsun@hit.edu.cn (J.-L. Sun).

0997-7538/$ – see front matter
doi:10.1016/j.euromechsol.2004.05.005

tween two cracks in a piezoelectric medium under incident anti-plane shear waves loading. They also investigated the dynamic behavior of piezoelectric materials containing interacting cracks under anti-plane mechanical and in-plane electric loading (Wang and Meguid, 2000). Many piezoelectric devices are multi-layered by dissimilar piezoelectric materials, and they are susceptible to cracking due to uneven stress distributions. Following the dynamic theory of linear piezoelectricity, Shindo et al. (2002) considered the scattering of horizontally polarized shear waves from a single piezoelectric fiber partially bonded to an elastic matrix. The problem of interface cracks in piezoelectric materials can be found in works (Soh et al., 2000; Li and Tang, 2003; Zhou and Wang, 2002; Narita et al., 1999). Recently, Huang et al. (2002) studied the permeable multi-cracks problem in one kind of piezoelectric material strip subjected to dynamic anti-plane shear loading. However, the lengths of cracks are the same and cracks are not interface cracks. According to the authors' knowledge, the dynamic electro-elastic behavior of two pairs unequal parallel permeable interface cracks has not been studied.

In this paper, the scattering of anti-plane shear waves in piezoelectric materials with two pairs of unequal parallel interface cracks is considered by use of Schmidt method. By use of the Fourier transform, the problem could be solved with two pairs of dual integral equations in which the unknown variables are the jumps of the displacements across the crack surfaces. To solve the dual integral equations, the jumps of the displacements across the crack surfaces were expanded in two series of Jacobi polynomials. This process is quite different from those adopted in the references mentioned above. Some numerical results are presented graphically to show the effects of the geometric parameters, the frequency of the incident waves and materials properties on the dynamic stress and electric displacement intensity factors.

2. Statement of the problem

Consider an infinitely long piezoelectric layer with $2h$ in thickness bonded to two dissimilar piezoelectric half planes subjected to harmonic anti-plane shear waves, as shown in Fig. 1. Here, Cartesian coordinates (x, y, z) are the principal axes of the material symmetry, while the z-axis is oriented in the poling direction of the piezoelectric materials. It is assumed that two pairs of unequal parallel Griffith interface cracks with different lengths $(2a, 2b)$ are located along the bonding line. Consider one pair of cracks located from $l-a$ to $l+a$ at $y=h$ and from $l-b$ to $l+b$ at $y=-h$, with respect to the rectangular coordinates (x, y), and the other pair located from $-l-a$ to $-l+a$ at $y=h$ and from $-l-b$ to $-l+b$ at $y=-h$. In the present study, the harmonic anti-plane shear waves is vertically incident. The mechanical field corresponding to a time harmonic waves can be expressed in terms of the frequency ω, such that $\tau_{yz}(x, y, t) = \tau_0 \exp[-\mathrm{i}\omega t]$. Because the time dependence of all field quantities assumed to be of the form $\exp[-\mathrm{i}\omega t]$ is a common factor in all equations, it will be suppressed. We only consider that τ_0 is positive. Body forces and the free charges are ignored in the present work.

The dynamic anti-plane governing differential equations for piezoelectric materials in absence of body forces and free charges can be expressed as follows

$$c_{44}^{(k)} \nabla^2 w^{(k)} + e_{15}^{(k)} \nabla^2 \phi^{(k)} = \rho^{(k)} \frac{\partial^2 w^{(k)}}{\partial t^2}, \tag{1}$$

$$e_{15}^{(k)} \nabla^2 w^{(k)} - \varepsilon_{11}^{(k)} \nabla^2 \phi^{(k)} = 0 \tag{2}$$

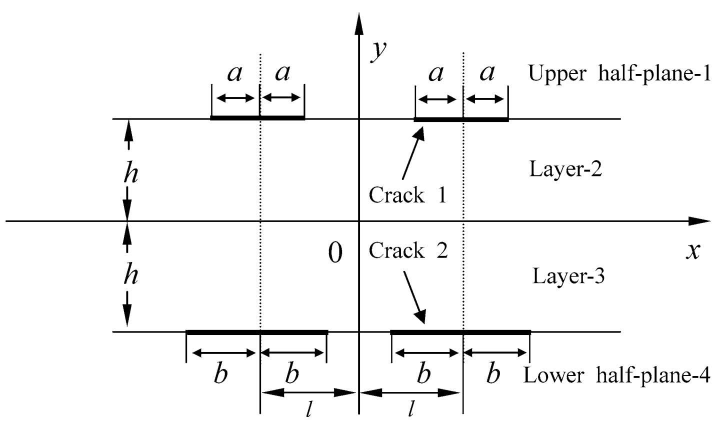

Fig. 1. Two pairs of unequal parallel interface cracks in piezoelectric materials.

in which $w^{(k)}$ and $\phi^{(k)}$ are the mechanical displacement and the electric potential, and $\rho^{(k)}$ is the mass density of piezoelectric materials, $c_{44}^{(k)}$ is the elastic stiffness measured in a constant electric field, $e_{15}^{(k)}$ is the piezoelectric constant and $\varepsilon_{11}^{(k)}$ is the dielectric permittivity measured at a uniform strain of the piezoelectric materials, while $\nabla^2 = \partial^2/\partial x^2 + \partial^2/\partial y^2$ is the two-dimensional Laplace operator. The superscript k $(k = 1, 2, 3, 4)$ refers to the upper half plane-1, the layer-2, the layer-3 and the lower half plane-4 as shown in Fig. 1, respectively.

The constitutive equations of the piezoelectric materials are

$$\tau_{jz}^{(k)} = c_{44}^{(k)} w_{,j}^{(k)} + e_{15}^{(k)} \phi_{,j}^{(k)}, \tag{3}$$

$$D_j^{(k)} = e_{15}^{(k)} w_{,j}^{(k)} - \varepsilon_{11}^{(k)} \phi_{,j}^{(k)}, \tag{4}$$

where $\tau_{jz}^{(k)}$, $w_{,j}^{(k)}$, $\phi_{,j}^{(k)}$ and $D_j^{(k)}$ $(j = x, y)$ are the stress, strain, electric field strength and electric displacement tensors, respectively.

As discussed in reference (Soh et al., 2000), since the opening displacement is zero for the present anti-plane shear problem, the crack surfaces can be assumed to be in perfect contact. Accordingly, both the electric potential and normal electric displacement are assumed to be continuous across the crack surfaces. Therefore, in this paper, we obtain the permeable electric boundary condition. Similar to the work (Narita and Shindo, 1998), the boundary conditions of the present problem can be stated below:

$$\begin{aligned} &\tau_{yz}^{(1)}(x,h) = \tau_{yz}^{(2)}(x,h), \qquad \phi^{(1)}(x,h) = \phi^{(2)}(x,h), \\ &D_y^{(1)}(x,h) = D_y^{(2)}(x,h) \quad \big(|x| \geqslant 0\big), \end{aligned} \tag{5a-c}$$

$$\begin{aligned} &w^{(2)}(x,0) = w^{(3)}(x,0), \qquad \tau_{yz}^{(2)}(x,0) = \tau_{yz}^{(3)}(x,0), \\ &\phi^{(2)}(x,0) = \phi^{(3)}(x,0), \quad D_y^{(2)}(x,0) = D_y^{(3)}(x,0) \quad \big(|x| \geqslant 0\big), \end{aligned} \tag{6a-d}$$

$$\begin{aligned} &\tau_{yz}^{(3)}(x,-h) = \tau_{yz}^{(4)}(x,-h), \qquad \phi^{(3)}(x,-h) = \phi^{(4)}(x,-h), \\ &D_y^{(3)}(x,-h) = D_y^{(4)}(x,-h) \quad \big(|x| \geqslant 0\big), \end{aligned} \tag{7a-c}$$

$$\tau_{yz}^{(1)}(x,h) = \tau_{yz}^{(2)}(x,h) = -\tau_0 \quad \big(l - a \leqslant |x| \leqslant l + a\big), \tag{8}$$

$$\tau_{yz}^{(3)}(x,-h) = \tau_{yz}^{(4)}(x,-h) = -\tau_0 \exp\left[\mathrm{i}\omega \frac{2h}{c^{(2)}}\right] \quad \big(l - b \leqslant |x| \leqslant l + b\big), \tag{9}$$

$$w^{(1)}(x,h) = w^{(2)}(x,h) \quad \big(0 \leqslant |x| < l - a,\ |x| > l + a\big), \tag{10}$$

$$w^{(3)}(x,-h) = w^{(4)}(x,-h) \quad \big(0 \leqslant |x| < l - b, |x| > l + b\big). \tag{11}$$

3. Solution of the problem

Owing to the symmetry in geometry and loading, it's sufficient to consider only the right side of the planes, $x \geqslant 0$ and $-\infty < y < \infty$. Assume that the solution of Eqs. (1) and (2) as following integrals:

$$\begin{cases} w^{(1)}(x,y) = \dfrac{2}{\pi}\displaystyle\int_0^\infty A_1(s)\,\mathrm{e}^{-\gamma^{(1)}y}\cos(sx)\,\mathrm{d}s, \\ \phi^{(1)}(x,y) = \dfrac{e_{15}^{(1)}}{\varepsilon_{11}^{(1)}} w^{(1)}(x,y) + \dfrac{2}{\pi}\displaystyle\int_0^\infty C_1(s)\,\mathrm{e}^{-sy}\cos(sx)\,\mathrm{d}s, \end{cases} \tag{12}$$

$$\begin{cases} w^{(2)}(x,y) = \dfrac{2}{\pi}\displaystyle\int_0^\infty \big[A_2(s)\,\mathrm{e}^{-\gamma^{(2)}y} + B_2(s)\,\mathrm{e}^{\gamma^{(2)}y}\big]\cos(sx)\,\mathrm{d}s, \\ \phi^{(2)}(x,y) = \dfrac{e_{15}^{(2)}}{\varepsilon_{11}^{(2)}} w^{(2)}(x,y) + \dfrac{2}{\pi}\displaystyle\int_0^\infty \big[C_2(s)\,\mathrm{e}^{-sy} + D_2(s)\,\mathrm{e}^{sy}\big]\cos(sx)\,\mathrm{d}s, \end{cases} \tag{13}$$

$$\begin{cases} w^{(3)}(x,y)=\dfrac{2}{\pi}\displaystyle\int_0^\infty\big[A_3(s)\,\mathrm{e}^{\gamma^{(2)}y}+B_3(s)\,\mathrm{e}^{-\gamma^{(2)}y}\big]\cos(sx)\,\mathrm{d}s,\\ \phi^{(3)}(x,y)=\dfrac{e_{15}^{(2)}}{\varepsilon_{11}^{(2)}}w^{(3)}(x,y)+\dfrac{2}{\pi}\displaystyle\int_0^\infty\big[C_3(s)\,\mathrm{e}^{sy}+D_3(s)\,\mathrm{e}^{-sy}\big]\cos(sx)\,\mathrm{d}s, \end{cases}\tag{14}$$

$$\begin{cases} w^{(4)}(x,y)=\dfrac{2}{\pi}\displaystyle\int_0^\infty A_4(s)\,\mathrm{e}^{\gamma^{(1)}y}\cos(sx)\,\mathrm{d}s,\\ \phi^{(4)}(x,y)=\dfrac{e_{15}^{(1)}}{\varepsilon_{11}^{(1)}}w^{(4)}(x,y)+\dfrac{2}{\pi}\displaystyle\int_0^\infty C_4(s)\,\mathrm{e}^{sy}\cos(sx)\,\mathrm{d}s, \end{cases}\tag{15}$$

where ${\gamma^{(J)}}^2=s^2-\omega^2/{c^{(J)}}^2$, subscript J $(J=1,2)$ stands for piezoelectric materials. $A_k(s)$ $(k=1,2,3,4)$, $B_k(s)$ $(k=2,3)$, $C_k(s)$ $(k=1,2,3,4)$, $D_k(s)$ $(k=2,3)$ are unknown functions to be determined from the boundary conditions.

By virtue of constitutive equations (3) and (4), we can obtain the expressions for the stress and electric displacement fields

$$\begin{cases} \tau_{yz}^{(1)}=-\dfrac{2}{\pi}\displaystyle\int_0^\infty\big[\mu^{(1)}\gamma^{(1)}A_1(s)\,\mathrm{e}^{-\gamma^{(1)}y}+e_{15}^{(1)}sC_1(s)\,\mathrm{e}^{-sy}\big]\cos(sx)\,\mathrm{d}s,\\ D_y^{(1)}=\dfrac{2}{\pi}\displaystyle\int_0^\infty\varepsilon_{11}^{(1)}sC_1(s)\,\mathrm{e}^{-sy}\cos(sx)\,\mathrm{d}s, \end{cases}\tag{16}$$

$$\begin{cases} \tau_{yz}^{(2)}=-\dfrac{2}{\pi}\displaystyle\int_0^\infty\big\{\mu^{(2)}\gamma^{(2)}\big[A_2(s)\,\mathrm{e}^{-\gamma^{(2)}y}-B_2(s)\,\mathrm{e}^{\gamma^{(2)}y}\big]+e_{15}^{(2)}s\big[C_2(s)\,\mathrm{e}^{-sy}-D_2(s)\,\mathrm{e}^{sy}\big]\big\}\cos(sx)\,\mathrm{d}s,\\ D_y^{(2)}=\dfrac{2}{\pi}\displaystyle\int_0^\infty\varepsilon_{11}^{(2)}s\big[C_2(s)\,\mathrm{e}^{-sy}-D_2(s)\,\mathrm{e}^{sy}\big]\cos(sx)\,\mathrm{d}s, \end{cases}\tag{17}$$

$$\begin{cases} \tau_{yz}^{(3)}=\dfrac{2}{\pi}\displaystyle\int_0^\infty\big\{\mu^{(2)}\gamma^{(2)}\big[A_3(s)\,\mathrm{e}^{\gamma^{(2)}y}-B_3(s)\,\mathrm{e}^{-\gamma^{(2)}y}\big]+e_{15}^{(2)}s\big[C_3(s)\,\mathrm{e}^{sy}-D_3(s)\,\mathrm{e}^{-sy}\big]\big\}\cos(sx)\,\mathrm{d}s,\\ D_y^{(3)}=-\dfrac{2}{\pi}\displaystyle\int_0^\infty\varepsilon_{11}^{(2)}s\big[C_3(s)\,\mathrm{e}^{sy}-D_3(s)\,\mathrm{e}^{-sy}\big]\cos(sx)\,\mathrm{d}s, \end{cases}\tag{18}$$

$$\begin{cases} \tau_{yz}^{(4)}=\dfrac{2}{\pi}\displaystyle\int_0^\infty\big[\mu^{(1)}\gamma^{(1)}A_4(s)\,\mathrm{e}^{\gamma^{(1)}y}+e_{15}^{(1)}sC_4(s)\,\mathrm{e}^{sy}\big]\cos(sx)\,\mathrm{d}s,\\ D_y^{(4)}=-\dfrac{2}{\pi}\displaystyle\int_0^\infty\varepsilon_{11}^{(1)}sC_4(s)\,\mathrm{e}^{sy}\cos(sx)\,\mathrm{d}s. \end{cases}\tag{19}$$

To get the functions $A_k(s)$, $B_k(s)$, $C_k(s)$ and $D_k(s)$, the gap functions of the crack surface displacements and the electric potentials are defined as follows

$$f_{w1}(x)=w^{(1)}(x,h)-w^{(2)}(x,h),\tag{20}$$

$$f_{w2}(x)=w^{(3)}(x,-h)-w^{(4)}(x,-h),\tag{21}$$

$$f_{\phi1}(x)=\phi^{(1)}(x,h)-\phi^{(2)}(x,h),\tag{22}$$

$$f_{\phi2}(x)=\phi^{(3)}(x,-h)-\phi^{(4)}(x,-h).\tag{23}$$

Substituting Eqs. (12)–(15) into Eqs. (20)–(23), and applying Fourier cosine transforms (a superposed bar indicates the Fourier cosine transforms throughout the paper) with the boundary conditions (5), (7), (10) and (11), it can be obtained

$$\overline{f_{w1}}(s) = A_1(s)\,\mathrm{e}^{-\gamma^{(1)}h} - A_2(s)\,\mathrm{e}^{-\gamma^{(2)}h} - B_2(s)\,\mathrm{e}^{\gamma^{(2)}h}, \tag{24}$$

$$\overline{f_{w2}}(s) = A_3(s)\,\mathrm{e}^{-\gamma^{(2)}h} + B_3(s)\,\mathrm{e}^{\gamma^{(2)}h} - A_4(s)\,\mathrm{e}^{-\gamma^{(1)}h}, \tag{25}$$

$$\overline{f_{\phi 1}}(s) = \frac{e_{15}^{(1)}}{\varepsilon_{11}^{(1)}} A_1(s)\,\mathrm{e}^{-\gamma^{(1)}h} + C_1(s)\,\mathrm{e}^{-sh} - \frac{e_{15}^{(2)}}{\varepsilon_{11}^{(2)}}\bigl[A_2(s)\,\mathrm{e}^{-\gamma^{(2)}h} + B_2(s)\,\mathrm{e}^{\gamma^{(2)}h}\bigr] - \bigl[C_2(s)\,\mathrm{e}^{-sh} + D_2(s)\,\mathrm{e}^{sh}\bigr] = 0, \tag{26}$$

$$\overline{f_{\phi 2}}(s) = \frac{e_{15}^{(2)}}{\varepsilon_{11}^{(2)}}\bigl[A_3(s)\,\mathrm{e}^{-\gamma^{(2)}h} + B_3(s)\,\mathrm{e}^{\gamma^{(2)}h}\bigr] + \bigl[C_3(s)\,\mathrm{e}^{-sh} + D_3(s)\,\mathrm{e}^{sh}\bigr] - \frac{e_{15}^{(1)}}{\varepsilon_{11}^{(1)}} A_4(s)\,\mathrm{e}^{-\gamma^{(1)}h} - C_4(s)\,\mathrm{e}^{-sh} = 0. \tag{27}$$

By applying Fourier cosine transforms to Eqs. (16)–(19) with boundary (5)–(11), it can be obtained

$$\mu^{(1)}\gamma^{(1)}A_1(s)\,\mathrm{e}^{-\gamma^{(1)}h} + e_{15}^{(1)} s C_1(s)\,\mathrm{e}^{-sh} = \mu^{(2)}\gamma^{(2)}\bigl\lfloor A_2(s)\,\mathrm{e}^{-\gamma^{(2)}h} - B_2(s)\,\mathrm{e}^{\gamma^{(2)}h}\bigr\rfloor + e_{15}^{(2)} s\bigl[C_2(s)\,\mathrm{e}^{-sh} - D_2(s)\,\mathrm{e}^{sh}\bigr], \tag{28}$$

$$\mu^{(2)}\gamma^{(2)}\bigl\lfloor A_3(s)\,\mathrm{e}^{-\gamma^{(2)}h} - B_3(s)\,\mathrm{e}^{\gamma^{(2)}h}\bigr\rfloor + e_{15}^{(2)} s\bigl[C_3(s)\,\mathrm{e}^{-sh} - D_3(s)\,\mathrm{e}^{sh}\bigr] = \mu^{(1)}\gamma^{(1)}A_4(s)\,\mathrm{e}^{-\gamma^{(1)}h} + e_{15}^{(1)} s C_4(s)\,\mathrm{e}^{-sh}, \tag{29}$$

$$\varepsilon_{11}^{(1)} C_1(s)\,\mathrm{e}^{-sh} = \varepsilon_{11}^{(2)}\bigl\lfloor C_2(s)\,\mathrm{e}^{-sh} - D_2(s)\,\mathrm{e}^{sh}\bigr\rfloor, \tag{30}$$

$$\varepsilon_{11}^{(2)}\bigl\lfloor C_3(s)\,\mathrm{e}^{-sh} - D_3(s)\,\mathrm{e}^{sh}\bigr\rfloor = \varepsilon_{11}^{(1)} C_4(s)\,\mathrm{e}^{-sh}, \tag{31}$$

$$A_2(s) + B_2(s) = A_3(s) + B_3(s), \qquad A_2(s) - B_2(s) = -A_3(s) + B_3(s), \tag{32}$$

$$C_2(s) + D_2(s) = C_3(s) + D_3(s), \qquad C_2(s) - D_2(s) = -C_3(s) + D_3(s). \tag{33}$$

By solving twelve Eqs. (24)–(33) with twelve unknown functions $A_k(s)$, $B_k(s)$, $C_k(s)$, $D_k(s)$, and substituting the solutions into Eqs. (16) and (19) and applying the boundary conditions (5), (7)–(9), it can be obtained

$$\frac{2}{\pi}\int_0^\infty \overline{f_{w1}}(s)\cos(sx)\,\mathrm{d}s = 0, \quad 0 \leqslant x < l-a \text{ and } x > l+a, \tag{34}$$

$$\frac{2}{\pi}\int_0^\infty \overline{f_{w2}}(s)\cos(sx)\,\mathrm{d}s = 0, \quad 0 \leqslant x < l-b \text{ and } x > l+b, \tag{35}$$

$$\frac{2}{\pi}\int_0^\infty s\bigl[\alpha(s)\overline{f_{w1}}(s) + \beta(s)\overline{f_{w2}}(s)\bigr]\cos(sx)\,\mathrm{d}s = -\tau_0, \quad l-a \leqslant x \leqslant l+a, \tag{36}$$

$$\frac{2}{\pi}\int_0^\infty s\bigl[\beta(s)\overline{f_{w1}}(s) + \alpha(s)\overline{f_{w2}}(s)\bigr]\cos(sx)\,\mathrm{d}s = -\tau_0 \exp\left[\mathrm{i}\omega\frac{2h}{c^{(2)}}\right], \quad l-b \leqslant x \leqslant l+b, \tag{37}$$

where $\alpha(s)$ and $\beta(s)$ are known functions and given in Appendix A.

4. Solution of the dual Integral equations

The set of dual integral equations (34)–(37) may be solved by use of the Schmidt method. The gap functions of the crack surface displacements are represented by the following series

$$f_{w1}(x) = \sum_{n=0}^{\infty} a_n P_n^{(1/2,1/2)}\left(\frac{x-l}{a}\right)\left(1 - \frac{(x-l)^2}{a^2}\right)^{1/2}, \quad \text{for } l-a \leqslant x \leqslant l+a,\ y = h, \tag{38a}$$

$$f_{w2}(x)=\sum_{n=0}^{\infty} b_n P_n^{(1/2,1/2)}\left(\frac{x-l}{b}\right)\left(1-\frac{(x-l)^2}{b^2}\right)^{1/2}, \quad \text{for } l-b\leqslant x\leqslant l+b,\ y=-h, \tag{38b}$$

where a_n and b_n is unknown coefficients to be determined and $P_n^{(1/2,1/2)}(x)$ is a Jacobi polynomial (Gradshteyn and Ryzhik, 1980). The Fourier cosine transforms of Eq. (38) are (Erdelyi, 1954)

$$\overline{f_{w1}}(s)=\frac{1}{s}\sum_{n=0}^{\infty} a_n R_n G_n(s) J_{n+1}(sa), \tag{39a}$$

$$\overline{f_{w2}}(s)=\frac{1}{s}\sum_{n=0}^{\infty} b_n R_n G_n(s) J_{n+1}(sb) \tag{39b}$$

in which

$$R_n=2\sqrt{\pi}\frac{\Gamma(n+1+1/2)}{n!}, \qquad G_n(s)=\begin{cases}(-1)^{n/2}\cos(sl), & n=0,2,4,6,\ldots,\\ (-1)^{(n+1)/2}\sin(sl), & n=1,3,5,7,\ldots,\end{cases}$$

$\Gamma(x)$ and $J_n(x)$ are Gamma and Bessel functions, respectively.

Substituting Eq. (39) into Eqs. (34)–(37), Eqs. (34) and (35) have been automatically satisfied. Integration with respect to x in $[l-a,x]$ and $[l-b,x]$, Eqs. (36) and (37) reduce to

$$\sum_{n=0}^{\infty} a_n R_n \int_0^{\infty} \frac{1}{s}\alpha(s)G_n(s)J_{n+1}(sa)\big[\sin(sx)-\sin(sl-sa)\big]\,\mathrm{d}s + \sum_{n=0}^{\infty} b_n R_n \int_0^{\infty} \frac{1}{s}\beta(s)G_n(s)J_{n+1}(sb)\big[\sin(sx)-\sin(sl-sa)\big]\,\mathrm{d}s=-\frac{\pi\tau_0}{2}(x-l+a), \tag{40a}$$

$$\sum_{n=0}^{\infty} a_n R_n \int_0^{\infty} \frac{1}{s}\beta(s)G_n(s)J_{n+1}(sa)\big[\sin(sx)-\sin(sl-sb)\big]\,\mathrm{d}s + \sum_{n=0}^{\infty} b_n R_n \int_0^{\infty} \frac{1}{s}\alpha(s)G_n(s)J_{n+1}(sb)\big[\sin(sx)-\sin(sl-sb)\big]\,\mathrm{d}s=-\frac{\pi\tau_0}{2}\exp\left[\mathrm{i}\omega\frac{2h}{c^{(2)}}\right](x-l+b). \tag{40b}$$

Eq. (40) can now be solved for the coefficients a_n and b_n by the Schmidt method such as in the works (Itou, 2001; Zhou et al., 1998). The Schmidt method is omitted in the present paper.

5. Intensity factors

The coefficients a_n and b_n are known, so that the entire stress and the electric displacement fields can be obtained. Stress $\tau_{yz}^{(k)}$ and electric displacement $D_y^{(k)}$ along the cracks lines can be expressed as

$$\tau_{yz}^{(1)}(x,h)=\tau_{yz}^{(2)}(x,h)=\frac{2}{\pi}\sum_{n=0}^{\infty} a_n R_n \int_0^{\infty}\big\{\alpha_c+\big[\alpha(s)-\alpha_c\big]\big\}G_n(s)J_{n+1}(sa)\cos(sx)\,\mathrm{d}s + \frac{2}{\pi}\sum_{n=0}^{\infty} b_n R_n \int_0^{\infty}\beta(s)G_n(s)J_{n+1}(sb)\cos(sx)\,\mathrm{d}s, \tag{41a}$$

$$\tau_{yz}^{(3)}(x,-h)=\tau_{yz}^{(4)}(x,-h)=\frac{2}{\pi}\sum_{n=1}^{\infty} b_n R_n \int_0^{\infty}\big\{\alpha_c+\big[\alpha(s)-\alpha_c\big]\big\}G_n(s)J_{2n-1}(sb)\cos(sx)\,\mathrm{d}s + \frac{2}{\pi}\sum_{n=0}^{\infty} a_n R_n \int_0^{\infty}\beta(s)G_n(s)J_{n+1}(sa)\cos(sx)\,\mathrm{d}s, \tag{41b}$$

$$D_y^{(1)}(x,h)=D_y^{(2)}(x,h)=\frac{2}{\pi}\sum_{n=0}^{\infty}a_nR_n\int_0^{\infty}\left\{\delta_c+\left[\delta(s)-\delta_c\right]\right\}G_n(s)J_{n+1}(sa)\cos(sx)\,\mathrm{d}s$$
$$+\frac{2}{\pi}\sum_{n=0}^{\infty}b_nR_n\int_0^{\infty}\gamma(s)G_n(s)J_{2n-1}(sb)\cos(sx)\,\mathrm{d}s, \tag{41c}$$

$$D_y^{(3)}(x,-h)=D_y^{(4)}(x,-h)=\frac{2}{\pi}\sum_{n=0}^{\infty}b_nR_n\int_0^{\infty}\left\{\delta_c+\left[\delta(s)-\delta_c\right]\right\}G_n(s)J_{n+1}(sb)\cos(sx)\,\mathrm{d}s$$
$$+\frac{2}{\pi}\sum_{n=0}^{\infty}a_nR_n\int_0^{\infty}\gamma(s)J_{n+1}(sa)G_n(s)\cos(sx)\,\mathrm{d}s, \tag{41d}$$

where $\gamma(s)$, $\delta(s)$, α_c and δ_c are known functions and given in Appendix A.

From the relationships (Gradshteyn and Ryzhik, 1980)

$$\int_0^{\infty}J_n(s\xi)\sin(s\psi)\,\mathrm{d}s=\begin{cases}\dfrac{\sin[n\sin^{-1}(\psi/\xi)]}{\sqrt{\xi^2-\psi^2}}, & \xi>\psi,\\[2mm] \dfrac{\xi^n\cos(n\pi/2)}{\sqrt{\psi^2-\xi^2}[\psi+\sqrt{\psi^2-\xi^2}]^n}, & \psi>\xi,\end{cases} \tag{42a}$$

$$\int_0^{\infty}J_n(s\xi)\cos(s\psi)\,\mathrm{d}s=\begin{cases}\dfrac{\cos[n\sin^{-1}(\psi/\xi)]}{\sqrt{\xi^2-\psi^2}}, & \xi>\psi,\\[2mm] -\dfrac{\xi^n\sin(n\pi/2)}{\sqrt{\psi^2-\xi^2}[\psi+\sqrt{\psi^2-\xi^2}]^n}, & \psi>\xi.\end{cases} \tag{42b}$$

The singular parts of the stress fields and the singular parts of the electric displacements in Eq. (41) can be expressed respectively as follows:

$$\tau^{(1)}=\tau^{(2)}=\frac{\alpha_c}{\pi}\sum_{n=0}^{\infty}a_nR_nH_n(a,x),\qquad \tau^{(3)}=\tau^{(4)}=\frac{\alpha_c}{\pi}\sum_{n=0}^{\infty}b_nR_nH_n(b,x), \tag{43a}$$

$$D^{(1)}=D^{(2)}=\frac{\delta_c}{\pi}\sum_{n=0}^{\infty}a_nR_nH_n(a,x),\qquad D^{(3)}=D^{(4)}=\frac{\delta_c}{\pi}\sum_{n=0}^{\infty}b_nR_nH_n(b,x), \tag{43b}$$

where $H_n(a,x)$, $H_n(b,x)$ are known functions and given in Appendix B.

We obtain the dynamic stress intensity factors (DSIFs) K_{aL}, K_{aR}, K_{bL} and K_{bR} as

$$K_{aL}=\lim_{x\to(l-a)^-}\sqrt{2\pi\left[(l-a)-x\right]}\tau^{(1)}=-\frac{\alpha_c}{\sqrt{\pi a}}\sum_{n=0}^{\infty}(-1)^na_nR_n, \tag{44a}$$

$$K_{aR}=\lim_{x\to(l+a)^+}\sqrt{2\pi\left[x-(l+a)\right]}\tau^{(1)}=-\frac{\alpha_c}{\sqrt{\pi a}}\sum_{n=0}^{\infty}a_nR_n, \tag{44b}$$

$$K_{bL}=\lim_{x\to(l-b)^-}\sqrt{2\pi\left[(l-b)-x\right]}\tau^{(4)}=-\frac{\alpha_c}{\sqrt{\pi b}}\sum_{n=0}^{\infty}(-1)^nb_nR_n, \tag{44c}$$

$$K_{bR}=\lim_{x\to(l+b)^+}\sqrt{2\pi\left[x-(l+b)\right]}\tau^{(4)}=-\frac{\alpha_c}{\sqrt{\pi b}}\sum_{n=0}^{\infty}b_nR_n. \tag{44d}$$

We obtain the dynamic electric displacement intensity factors D_{aL}, D_{aR}, D_{bL} and D_{bR} as

$$D_{aL}=\lim_{x\to(l-a)^-}\sqrt{2\pi\left[(l-a)-x\right]}D^{(1)}=-\frac{\delta_c}{\sqrt{\pi a}}\sum_{n=0}^{\infty}(-1)^na_nR_n=\frac{\delta_c}{\alpha_c}K_{aL}, \tag{45a}$$

$$D_{aR}=\lim_{x\to(l+a)^+}\sqrt{2\pi\left[x-(l+a)\right]}D^{(1)}=-\frac{\delta_c}{\sqrt{\pi a}}\sum_{n=0}^{\infty}a_nR_n=\frac{\delta_c}{\alpha_c}K_{aR}, \tag{45b}$$

$$D_{bL} = \lim_{x\to(l-b)^-} \sqrt{2\pi\big[(l-b)-x\big]}D^{(4)} = -\frac{\delta_c}{\sqrt{\pi b}} \sum_{n=0}^{\infty}(-1)^n b_n R_n = \frac{\delta_c}{\alpha_c} K_{bL}, \tag{45c}$$

$$D_{bR} = \lim_{x\to(l+b)^+} \sqrt{2\pi\big[x-(l+b)\big]}D^{(4)} = -\frac{\delta_c}{\sqrt{\pi b}} \sum_{n=0}^{\infty} b_n R_n = \frac{\delta_c}{\alpha_c} K_{bR}. \tag{45d}$$

From Eqs. (44) and (45), it can be seen that the dynamic electric displacement intensity factors can be obtained when the dynamic stress intensity factors were known.

6. Numerical calculations and discussion

To examine the effects of electro-mechanical interactions on the dynamic stress intensity factors and electric displacement intensity factors, we carried out numerical calculations for the piezoelectric ceramics PZT-4 and PZT-5H. The material constants of piezoelectric ceramics are list in Table 1.

The infinite series in Eq. (40) can be truncated by summing the first six terms. The values for left and right sides in Eq. (40a) are shown with $a/b = 1.0$, $h/b = 0.5$, $l/b = 1.1$ and $b\omega/c^{(1)} = 0.5$ in Table 2. Table 3 shows the values in Eq. (40b) for the same case. From the tables, it can be seen that the Schmidt method has been applied satisfactorily. The normalized DSIFs ($k_{al} = K_{aL}/(\sqrt{\pi a}\tau_0)$, $k_{ar} = K_{aR}/(\sqrt{\pi a}\tau_0)$, $k_{bl} = K_{bL}/(\sqrt{\pi b}\tau_0)$, $k_{br} = K_{bR}/(\sqrt{\pi b}\tau_0)$) are calculated numerically.

From the results in Figs. 2–9, the following observations are very significant:

Table 1
Material constants of piezoelectric ceramics

Materials	c_{44} ($\times 10^{10}$ N/m^2)	e_{15} (C/m^2)	ε_{11} ($\times 10^{-10}$ C/Vm)	ρ (kg/m^3)
PZT-4	2.56	12.7	64.6	7500
PZT-5H	2.3	17.0	150.4	7500

Table 2
Values of left and right equation (40a) for $a/b = 1.0$, $h/b = 0.5$, $l/b = 1.1$ and $b\omega/c^{(1)} = 0.5$

x	$\sum_{n=0}^{\infty} a_n E_n^*(x) + \sum_{n=0}^{\infty} b_n F_n^*(x)$	$U_0(x)/(-\pi\tau_0/2)$
0.3	$0.159996 - 0.146679 \times 10^{-5}$i	0.160000
0.5	$0.320039 + 0.149133 \times 10^{-4}$i	0.320000
0.7	$0.479981 - 0.744261 \times 10^{-5}$i	0.480000
0.9	$0.639972 - 0.109102 \times 10^{-4}$i	0.640000
1.1	$0.800013 + 0.488944 \times 10^{-5}$i	0.800000
1.3	$0.960028 + 0.106340 \times 10^{-4}$i	0.960000
1.5	$0.111999 - 0.307026 \times 10^{-5}$i	1.120000
1.7	$0.127997 - 0.104473 \times 10^{-4}$i	1.280000

Table 3
Values of left and right equation (40b) for $a/b = 1.0$, $h/b = 0.5$, $l/b = 1.1$ and $b\omega/c^{(1)} = 0.5$

x	$\sum_{n=0}^{\infty} a_n G_n^*(x) + \sum_{n=0}^{\infty} b_n H_n^*(x)$	$V_0(x)/(-\pi\tau_0/2)$
0.3	0.136633 + 0.083246i	0.136635 + 0.083252i
0.5	0.273295 + 0.166562i	0.273270 + 0.166504i
0.7	0.409893 + 0.249726i	0.409905 + 0.249756i
0.9	0.546522 + 0.332965i	0.546540 + 0.333007i
1.1	0.683183 + 0.416278i	0.683175 + 0.416259i
1.3	0.819828 + 0.499553i	0.819810 + 0.499511i
1.5	0.956440 + 0.582751i	0.956445 + 0.582763i
1.7	1.093060 + 0.665974i	1.093080 + 0.666015i

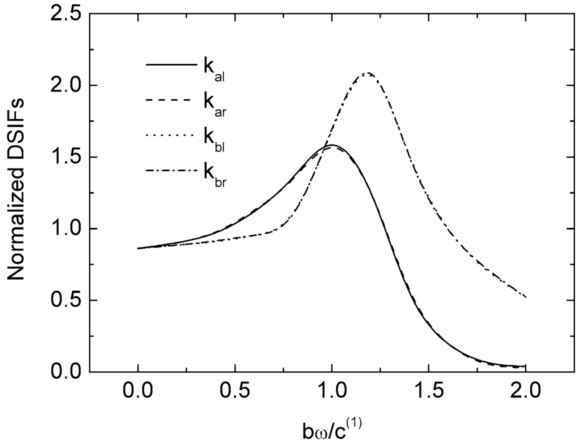

Fig. 2. The normalized DSIFs versus $b\omega/c^{(1)}$ ($a/b = 1.0$, $h/b = 0.5$, $l/b = 15$, elastic material).

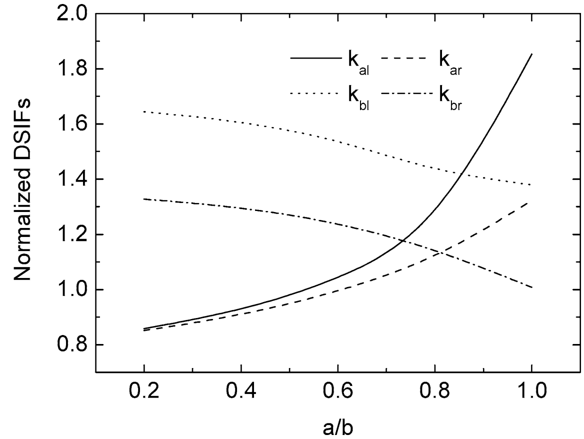

Fig. 3. The normalized DSIFs versus length of crack 1 ($l/b = 1.2$, $b\omega/c^{(1)} = 0.4$, $h/b = 0.5$, PZT-4/PZT-5H/PZT-4).

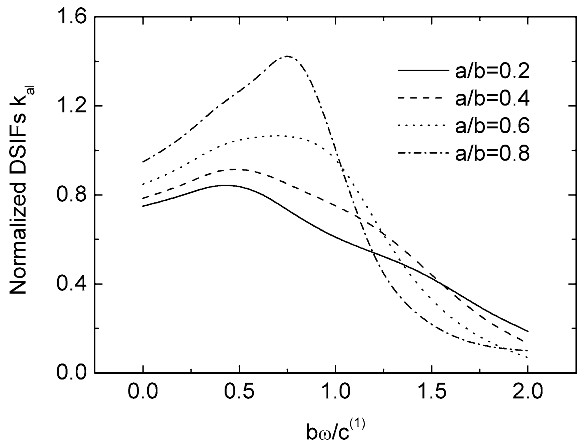

Fig. 4. The normalized DSIFs at left tip of crack 1 versus $b\omega/c^{(1)}$ for different a/b ($l/b = 1.2$, $h/b = 0.5$, PZT-4/PZT-5H/PZT-4).

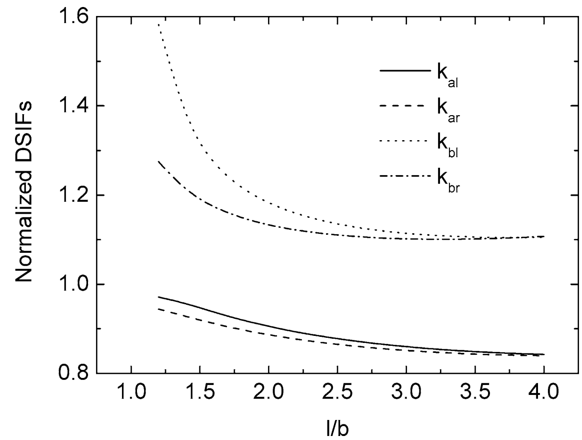

Fig. 5. The normalized DSIFs versus l/b ($b\omega/c^{(1)} = 0.4$, $a/b = 0.5$, $h/b = 0.5$, PZT-4/PZT-5H/PZT-4).

(1) Fig. 2 displays the variation of the normalized DSIFs with normalized wave number $b\omega/c^{(1)}$ for elastic material ($a/b = 1.0$, $h/b = 0.5$ and $l/b = 15$). The elastic solutions are obtained from the present formulation for piezoelectric materials by setting $c_{44}^{(1)} = c_{44}^{(2)}$ and $e_{15}^{(1)} = e_{15}^{(2)} = 0$. From this figure, it can be seen that the numerical results of normalized DSIFs agree closely with results investigated by Takakuda (1982) using the integral equation method. This implies the correctness and accuracy of our results.
(2) Fig. 3 exhibits the effect of the length of crack 1 on the normalized DSIFs for $l/b = 1.2$, $b\omega/c^{(1)} = 0.4$ and $h/b = 0.5$ (PZT-4/PZT-5H/PZT-4). It shows that the normalized DSIFs of crack 1 increase with increasing of a/b while those of the other one decrease, i.e. the normalized DSIFs of the crack 1 increase with the length of the crack 1. A similar phenomenon can be found in work (Zeng and Rajapakse, 2000). It is interesting to note that the normalized DSIFs at the left tips of cracks are always lager than those of the right ones.
(3) Fig. 4 shows the effect of length of crack 1 on the normalized DSIFs at left tip of crack 1 for different normalized wave numbers and different a/b ($l/b = 1.2$, $h/b = 0.5$ and PZT-4/PZT-5H/PZT-4). It should be noted that for lower frequencies ($b\omega/c^{(1)} < 1.0$) k_{al} increases with increasing of a/b. However, for higher frequencies, the effect of a/b becomes weak.
(4) Fig. 5 shows the effect of l/b on normalized DSIFs for $b\omega/c^{(1)} = 0.4$, $a/b = 0.5$ and $h/b = 0.5$ (PZT-4/PZT-5H/PZT-4). The normalized DSIFs decrease with increasing of the distance between two collinear cracks. The normalized DSIFs trend to steady values when $l/b > 3.5$. The reason is that the amplification effects between collinear cracks become weak.
(5) In Fig. 6, the normalized DSIFs versus h/b for $l/b = 1.2$, $a/b = 0.5$ and $b\omega/c^{(1)} = 0.4$ (PZT-4/PZT-5H/PZT-4) are shown. The magnitude of the normalized DSIFs of crack 1 increase with increasing of h/b. This is called shielding effect as

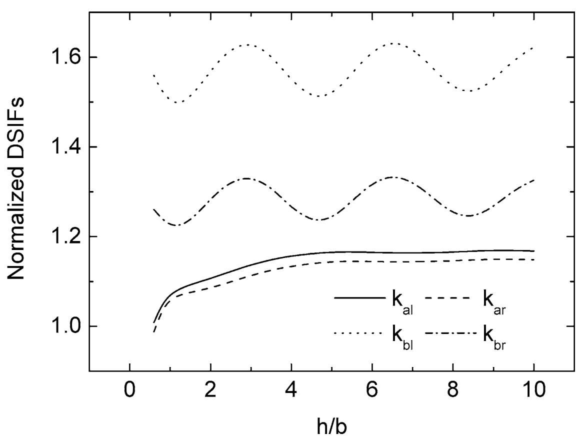

Fig. 6. The normalized stress intensity factors versus h ($l/b = 1.2$, $a/b = 0.5$, $b\omega/c^{(1)} = 0.4$, PZT-4/PZT-5H/PZT-4).

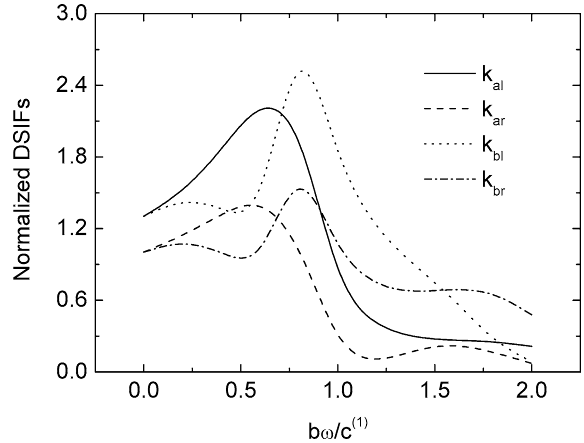

Fig. 7. The normalized DSIFs versus $b\omega/c^{(1)}$ ($l/b = 1.1$, $a/b = 1.0$, $h/b = 0.5$, PZT-4/PZT-5H/PZT-4).

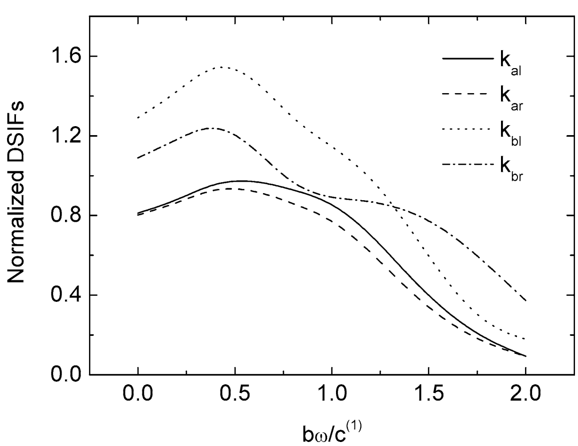

Fig. 8. The normalized DSIFs versus $b\omega/c^{(1)}$ ($l/b = 1.1$, $a/b = 0.5$, $h/b = 0.5$, PZT-4/PZT-5H/PZT-4).

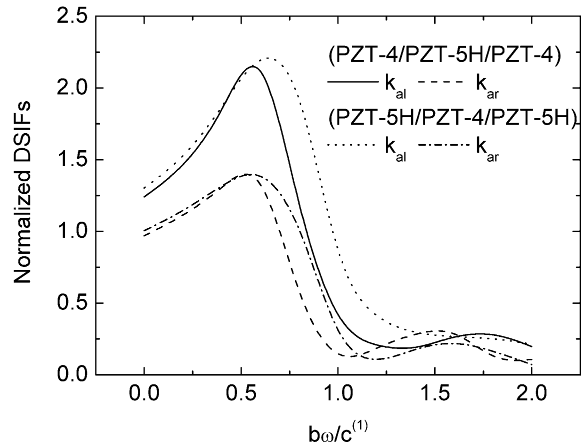

Fig. 9. The normalized DSIFs k_{al} and k_{ar} versus $b\omega/c^{(1)}$ ($l/b = 1.1$, $a/b = 0.5$, $h/b = 0.5$, PZT-4/PZT-5H/PZT-4 and PZT-5H/PZT-4/PZT-5H).

discussed in reference (Ratwani and Gupta, 1974). When $h/b > 4.0$, the normalized DSIFs of crack 1 trend to steady values. The shielding effect is very small when $h/b > 4.0$. However, the magnitude of the normalized DSIFs of crack 2 exhibits oscillations because the amplitude values of the loading on crack 2 varies with h/b.

(6) Figs. 7 and 8 show the effect of wave number $b\omega/c^{(1)}$ on the normalized DSIFs for $l/b = 1.1$, $h/b = 0.5$, $a/b = 1.0$ or $a/b = 0.5$ (PZT-4/PZT-5H/PZT-4). The normalized DSIFs increase with the increase of wave number $b\omega/c^{(1)}$, until reach peak values, and then decease with the increase of $b\omega/c^{(1)}$. From the results, it can be concluded that the stress concentration can be deduced by adjusting the frequency of incident waves in engineering practices. It can also be observed that the peak value occurs at different frequency for each crack. The present results show similar trends to those for materials without piezoelectric effect (Takakuda, 1982).

(7) Fig. 9 shows the effect of materials properties on the normalized DSIFs for $l/b = 1.1$, $a/b = 0.5$, $h/b = 0.5$ (PZT-4/PZT-5H/PZT-4 and PZT-5H/PZT-4/PZT-5H). It can be seen that, the results of normalized DSIFs for PZT-4/PZT-5H/PZT-4 are smaller than those for the other combination when $b\omega/c^{(1)} < 1.2$. The results reveal that the stress concentration can be adjusted by bonding different piezoelectric layer.

(8) Based on the numerical calculation outlined above, it can be concluded that the normalized DSIFs depend on the length of cracks, thickness of piezoelectric strip, frequency of incident wave and materials properties.

Acknowledgements

The authors wish to thank the National Natural Science Foundation of China (10172030 and 50232030) and the Natural Science Foundation of Hei Long Jiang Province (A0301).

Appendix A

$$\gamma^{(1)^2} = s^2 - \omega^2/c^{(1)^2}, \quad c^{(1)^2} = \mu^{(1)}/\rho^{(1)}, \quad \mu^{(1)} = c_{44}^{(1)} + e_{15}^{(1)^2}/\varepsilon_{11}^{(1)}, \quad \gamma_N^{(1)^2} = 1 - \omega^2/\big(c^{(1)^2}s^2\big),$$
$$\gamma^{(2)^2} = s^2 - \omega^2/c^{(2)^2}, \quad c^{(2)^2} = \mu^{(2)}/\rho^{(2)}, \quad \mu^{(2)} = c_{44}^{(2)} + e_{15}^{(2)^2}/\varepsilon_{11}^{(2)}, \quad \gamma_N^{(2)^2} = 1 - \omega^2/\big(c^{(2)^2}s^2\big),$$
$$H_1 = 1 + \mathrm{e}^{-4h\gamma^{(2)}}, \quad H_2 = 1 - \mathrm{e}^{-4h\gamma^{(2)}}, \quad H_3 = 1 + \mathrm{e}^{-4hs}, \quad H_4 = 1 - \mathrm{e}^{-4hs},$$
$$R_1 = 2H_1H_4 e_{15}^{(1)^3} e_{15}^{(2)} \gamma_N^{(2)} \mu^{(2)} \varepsilon_{11}^{(1)} \varepsilon_{11}^{(2)^3}, \qquad R_2 = -2H_1H_4 e_{15}^{(1)} e_{15}^{(2)} \gamma_N^{(1)} \gamma_N^{(2)} \mu^{(1)} \mu^{(2)} \varepsilon_{11}^{(1)^2} \varepsilon_{11}^{(2)^3},$$
$$R_3 = -H_1H_4 e_{15}^{(1)^2} \gamma_N^{(2)} \mu^{(2)} \varepsilon_{11}^{(2)^2} \big(e_{15}^{(2)^2} \varepsilon_{11}^{(1)^2} + \varepsilon_{11}^{(2)^2}\big(e_{15}^{(1)^2} - 2\gamma_N^{(1)} \mu^{(1)} \varepsilon_{11}^{(1)}\big)\big),$$
$$R_4 = H_1H_4 \gamma_N^{(1)} \gamma_N^{(2)} \mu^{(1)} \mu^{(2)} \varepsilon_{11}^{(1)^2} \varepsilon_{11}^{(2)^2} \big(2e_{15}^{(2)^2} \varepsilon_{11}^{(1)} - \gamma_N^{(1)} \mu^{(1)} \big(\varepsilon_{11}^{(1)^2} + \varepsilon_{11}^{(2)^2}\big)\big),$$
$$R_5 = 2H_1H_3 \gamma_N^{(1)} \gamma_N^{(2)} \mu^{(1)} \mu^{(2)} \varepsilon_{11}^{(1)^2} \varepsilon_{11}^{(2)} \big(e_{15}^{(2)^2} \varepsilon_{11}^{(1)^2} - e_{15}^{(1)} e_{15}^{(2)} \varepsilon_{11}^{(1)} \varepsilon_{11}^{(2)} + \varepsilon_{11}^{(2)^2} \big(e_{15}^{(1)^2} - \gamma_N^{(1)} \mu^{(1)} \varepsilon_{11}^{(1)}\big)\big),$$
$$R_6 = -H_2H_4 e_{15}^{(2)^4} \gamma_N^{(1)} \mu^{(1)} \varepsilon_{11}^{(1)^4}, \qquad R_7 = 2H_2H_4 e_{15}^{(1)} e_{15}^{(2)^3} \gamma_N^{(1)} \mu^{(1)} \varepsilon_{11}^{(1)^3} \varepsilon_{11}^{(2)},$$
$$R_8 = -H_2H_4 e_{15}^{(2)^2} \gamma_N^{(1)} \mu^{(1)} \varepsilon_{11}^{(1)^2} \varepsilon_{11}^{(2)^2} \big(e_{15}^{(1)^2} - \gamma_N^{(1)} \mu^{(1)} \varepsilon_{11}^{(1)}\big),$$
$$R_9 = H_2H_4 \gamma_N^{(2)^2} \mu^{(2)^2} \varepsilon_{11}^{(1)} \varepsilon_{11}^{(2)^2} \big(\gamma_N^{(1)} \mu^{(1)} \varepsilon_{11}^{(1)} \big(\varepsilon_{11}^{(1)^2} + \varepsilon_{11}^{(2)^2}\big) - e_{15}^{(1)^2} \varepsilon_{11}^{(2)^2}\big),$$
$$R_{10} = H_2H_3 \varepsilon_{11}^{(1)^2} \varepsilon_{11}^{(2)} \big(e_{15}^{(2)^2} \gamma_N^{(1)^2} \mu^{(1)^2} \varepsilon_{11}^{(1)^2} + \gamma_N^{(2)^2} \mu^{(2)^2} \varepsilon_{11}^{(2)^2} \big(e_{15}^{(1)^2} - 2\gamma_N^{(1)} \mu^{(1)} \varepsilon_{11}^{(1)}\big)\big),$$
$$R_{11} = -8\,\mathrm{e}^{-2h(\gamma^{(2)}+s)} e_{15}^{(2)} \gamma_N^{(1)} \gamma_N^{(2)} \mu^{(1)} \mu^{(2)} \varepsilon_{11}^{(1)^3} \varepsilon_{11}^{(2)} \big(e_{15}^{(2)} \varepsilon_{11}^{(1)} - e_{15}^{(1)} \varepsilon_{11}^{(2)}\big),$$
$$R = R_1 + R_2 + R_3 + R_4 + R_5 + R_6 + R_7 + R_8 + R_9 + R_{10} + R_{11},$$
$$S_1 = 2\,\mathrm{e}^{-2h\gamma^{(2)}}\,\mathrm{e}^{-4hs} \gamma_N^{(2)} \mu^{(2)} \varepsilon_{11}^{(1)^2} \big(-e_{15}^{(1)} e_{15}^{(2)} \varepsilon_{11}^{(1)} + \gamma_N^{(1)} \mu^{(1)} \varepsilon_{11}^{(1)} \big(\varepsilon_{11}^{(1)} - \varepsilon_{11}^{(2)}\big) + e_{15}^{(1)^2} \varepsilon_{11}^{(2)^2}\big),$$
$$S_2 = -2\,\mathrm{e}^{-4h\gamma^{(2)}}\,\mathrm{e}^{-2hs} \varepsilon_{11}^{(1)^2} \varepsilon_{11}^{(2)} \big(e_{15}^{(2)} \gamma_N^{(1)} \mu^{(1)} \varepsilon_{11}^{(1)} - e_{15}^{(1)} \gamma_N^{(2)} \mu^{(2)} \varepsilon_{11}^{(2)}\big)^2,$$
$$S_3 = 2\,\mathrm{e}^{-2hs} \varepsilon_{11}^{(1)^2} \varepsilon_{11}^{(2)} \big(e_{15}^{(2)} \gamma_N^{(1)} \mu^{(1)} \varepsilon_{11}^{(1)} + e_{15}^{(1)} \gamma_N^{(2)} \mu^{(2)} \varepsilon_{11}^{(2)}\big)^2,$$
$$S_4 = -2\,\mathrm{e}^{-2h\gamma^{(2)}} \gamma_N^{(2)} \mu^{(2)} \varepsilon_{11}^{(2)^2} \big(e_{15}^{(1)} e_{15}^{(2)} \varepsilon_{11}^{(1)} - e_{15}^{(1)^2} \varepsilon_{11}^{(2)} + \gamma_N^{(1)} \mu^{(1)} \varepsilon_{11}^{(1)} \big(\varepsilon_{11}^{(1)} + \varepsilon_{11}^{(2)}\big)\big)^2,$$
$$S = S_1 + S_2 + S_3 + S_4,$$
$$T_1 = H_2H_4 e_{15}^{(1)^3} \gamma_N^{(1)} \mu^{(1)} \varepsilon_{11}^{(1)^4} \varepsilon_{11}^{(2)}, \qquad T_2 = H_1H_4 e_{15}^{(1)^3} \gamma_N^{(2)} \mu^{(1)} \varepsilon_{11}^{(1)} \varepsilon_{11}^{(2)^4},$$
$$T_3 = -H_2 e_{15}^{(1)} \gamma_N^{(2)^2} \mu^{(2)^2} \varepsilon_{11}^{(1)^2} \varepsilon_{11}^{(2)^3} \big(\varepsilon_{11}^{(1)} H_3 - \varepsilon_{11}^{(2)} H_4\big), \qquad T_4 = -2H_1H_4 e_{15}^{(1)^2} e_{15}^{(2)} \gamma_N^{(2)} \mu^{(2)} \varepsilon_{11}^{(1)^2} \varepsilon_{11}^{(2)^3},$$
$$T_5 = -H_2 e_{15}^{(1)} \gamma_N^{(1)^2} \mu^{(1)^2} \varepsilon_{11}^{(1)^3} \varepsilon_{11}^{(2)^2} \big(\varepsilon_{11}^{(1)} H_3 - \varepsilon_{11}^{(2)} H_4\big), \qquad T_6 = H_2H_4 e_{15}^{(1)^2} e_{15}^{(2)} \gamma_N^{(1)} \mu^{(1)} \varepsilon_{11}^{(1)^2} \varepsilon_{11}^{(2)^3},$$
$$T_7 = -\big(H_3H_1 - 4\,\mathrm{e}^{-2h\gamma^{(2)}}\,\mathrm{e}^{-2hs}\big) e_{15}^{(2)} \gamma_N^{(1)} \gamma_N^{(2)} \mu^{(1)} \mu^{(2)} \varepsilon_{11}^{(1)^4} \varepsilon_{11}^{(2)^2},$$
$$T_8 = -H_1H_4 e_{15}^{(2)} \gamma_N^{(1)} \gamma_N^{(2)} \mu^{(1)} \mu^{(2)} \varepsilon_{11}^{(1)^3} \varepsilon_{11}^{(2)^3}, \qquad T_9 = -2H_2H_4 e_{15}^{(1)} e_{15}^{(2)^2} \gamma_N^{(1)} \mu^{(1)} \varepsilon_{11}^{(1)^3} \varepsilon_{11}^{(2)^2},$$
$$T_{10} = H_1H_4 e_{15}^{(1)} e_{15}^{(2)^2} \gamma_N^{(2)} \mu^{(2)} \varepsilon_{11}^{(1)^3} \varepsilon_{11}^{(2)^2}, \qquad T_{11} = -\big(H_3H_1 + 4\,\mathrm{e}^{-2h\gamma^{(2)}}\,\mathrm{e}^{-2hs}\big) e_{15}^{(1)} \gamma_N^{(1)} \gamma_N^{(2)} \mu^{(1)} \mu^{(2)} \varepsilon_{11}^{(1)^3} \varepsilon_{11}^{(2)^3},$$
$$T_{12} = -H_1H_4 e_{15}^{(1)} \gamma_N^{(1)} \gamma_N^{(2)} \mu^{(1)} \mu^{(2)} \varepsilon_{11}^{(1)^2} \varepsilon_{11}^{(2)^4},$$
$$T = T_1 + T_2 + T_3 + T_4 + T_5 + T_6 + T_7 + T_8 + T_9 + T_{10} + T_{11} + T_{12},$$
$$U_1 = 2\,\mathrm{e}^{-2h\gamma^{(2)}} e_{15}^{(1)} e_{15}^{(2)^2} \gamma_N^{(2)} \mu^{(2)} \varepsilon_{11}^{(1)^3} \varepsilon_{11}^{(2)^3},$$
$$U_2 = 2\,\mathrm{e}^{-4h\gamma^{(2)}}\,\mathrm{e}^{-2hs} \big(\gamma_N^{(1)} \mu^{(1)} - \gamma_N^{(2)} \mu^{(2)}\big) \varepsilon_{11}^{(1)^3} \varepsilon_{11}^{(2)^2} \big(e_{15}^{(2)} \gamma_N^{(1)} \mu^{(1)} \varepsilon_{11}^{(1)} - e_{15}^{(1)} \gamma_N^{(2)} \mu^{(2)} \varepsilon_{11}^{(2)}\big),$$

$$U_3 = -2\,\mathrm{e}^{-2hs}\big(\gamma_N^{(1)}\mu^{(1)} + \gamma_N^{(2)}\mu^{(2)}\big)\varepsilon_{11}^{(1)^3}\varepsilon_{11}^{(2)^2}\big(e_{15}^{(2)}\gamma_N^{(1)}\mu^{(1)}\varepsilon_{11}^{(1)} + e_{15}^{(1)}\gamma_N^{(2)}\mu^{(2)}\varepsilon_{11}^{(2)}\big),$$
$$U_4 = -2\,\mathrm{e}^{-2h\gamma^{(2)}}\,\mathrm{e}^{-4hs}\gamma_N^{(2)}\mu^{(2)}\varepsilon_{11}^{(1)}\varepsilon_{11}^{(2)^2}\big(e_{15}^{(2)}\varepsilon_{11}^{(1)} + e_{15}^{(1)}\varepsilon_{11}^{(2)}\big)\big(e_{15}^{(1)}e_{15}^{(2)}s\varepsilon_{11}^{(1)} - e_{15}^{(1)^2}s\varepsilon_{11}^{(2)}\big),$$
$$U_5 = 2\,\mathrm{e}^{-2h\gamma^{(2)}}e_{15}^{(1)}\gamma_N^{(2)}\mu^{(2)}\varepsilon_{11}^{(1)}\varepsilon_{11}^{(2)^3}\big(e_{15}^{(1)^2}\varepsilon_{11}^{(2)} - \gamma_N^{(1)}\mu^{(1)}\varepsilon_{11}^{(1)}\big(\varepsilon_{11}^{(1)} + \varepsilon_{11}^{(2)}\big)\big),$$
$$U_6 = 2\,\mathrm{e}^{-2h\gamma^{(2)}}\,e_{15}^{(2)}\gamma_N^{(2)}\mu^{(2)}\varepsilon_{11}^{(1)^2}\varepsilon_{11}^{(2)^2}\big(-2\,e_{15}^{(1)^2}\varepsilon_{11}^{(2)} + \gamma_N^{(1)}\mu^{(1)}\varepsilon_{11}^{(1)}\big(\varepsilon_{11}^{(1)} + \varepsilon_{11}^{(2)}\big)\big),$$
$$U_7 = -2\,\mathrm{e}^{-2h\gamma^{(2)}}\,\mathrm{e}^{-4hs}\gamma_N^{(1)}\gamma_N^{(2)}\mu^{(1)}\mu^{(2)}\varepsilon_{11}^{(1)^2}\varepsilon_{11}^{(2)^2}\big(e_{15}^{(2)}\varepsilon_{11}^{(1)} + e_{15}^{(1)}\varepsilon_{11}^{(2)}\big)\big(\varepsilon_{11}^{(2)} - \varepsilon_{11}^{(1)}\big),$$
$$U = U_1 + U_2 + U_3 + U_4 + U_5 + U_6 + U_7,$$
$$V_1 = H_2H_4e_{15}^{(2)^2}\varepsilon_{11}^{(1)^3}\big(e_{15}^{(2)}\varepsilon_{11}^{(1)} - 4e_{15}^{(1)}\varepsilon_{11}^{(2)}\big), \qquad V_2 = 2H_2H_4e_{15}^{(2)^2}\varepsilon_{11}^{(1)^2}\varepsilon_{11}^{(2)^2}\big(3e_{15}^{(1)^2} - \gamma_N^{(1)}\mu^{(1)}\varepsilon_{11}^{(1)}\big),$$
$$V_3 = 4H_2H_4e_{15}^{(1)}e_{15}^{(2)}\varepsilon_{11}^{(1)}\varepsilon_{11}^{(2)^3}\big(-e_{15}^{(1)^2} + \gamma_N^{(1)}\mu^{(1)}\varepsilon_{11}^{(1)}\big),$$
$$V_4 = H_2H_4\varepsilon_{11}^{(2)^2}\big(e_{15}^{(1)^4}\varepsilon_{11}^{(2)^2} - 2e_{15}^{(1)^2}\gamma_N^{(1)}\mu^{(1)}\varepsilon_{11}^{(1)}\varepsilon_{11}^{(2)^2} + \gamma_N^{(1)^2}\mu^{(1)^2}\varepsilon_{11}^{(1)^2}\big(\varepsilon_{11}^{(1)^2} + \varepsilon_{11}^{(2)^2}\big)\big),$$
$$V_5 = H_2H_4\gamma_N^{(2)^2}\mu^{(2)^2}\varepsilon_{11}^{(1)^2}\varepsilon_{11}^{(2)^2}\big(\varepsilon_{11}^{(1)^2} + \varepsilon_{11}^{(2)^2}\big),$$
$$V_6 = 8\,\mathrm{e}^{-2h\gamma^{(2)}}\,\mathrm{e}^{-2hs}\gamma_N^{(2)}\mu^{(2)}\varepsilon_{11}^{(1)^2}\varepsilon_{11}^{(2)}\big(e_{15}^{(2)}\varepsilon_{11}^{(1)} + e_{15}^{(1)}\varepsilon_{11}^{(2)}\big)^2,$$
$$V_7 = -2H_2H_3e_{15}^{(2)}\gamma_N^{(1)}\mu^{(1)}\varepsilon_{11}^{(1)^3}\varepsilon_{11}^{(2)}\big(e_{15}^{(2)}\varepsilon_{11}^{(1)} - 2e_{15}^{(1)}\varepsilon_{11}^{(2)}\big),$$
$$V_8 = 2H_2H_3\varepsilon_{11}^{(1)^2}\varepsilon_{11}^{(2)^3}\big(-e_{15}^{(1)^2}\gamma_N^{(1)}\mu^{(1)} + \gamma_N^{(1)^2}\mu^{(1)^2}\varepsilon_{11}^{(1)} + \gamma_N^{(2)^2}\mu^{(2)^2}\varepsilon_{11}^{(1)}\big),$$
$$V_9 = -2H_1H_4e_{15}^{(2)}\gamma_N^{(2)}\mu^{(2)}\varepsilon_{11}^{(1)^2}\varepsilon_{11}^{(2)^2}\big(e_{15}^{(2)}\varepsilon_{11}^{(1)} - 2e_{15}^{(1)}\varepsilon_{11}^{(2)}\big),$$
$$V_{10} = 2H_1H_4\gamma_N^{(2)}\mu^{(2)}\varepsilon_{11}^{(1)}\varepsilon_{11}^{(2)^2}\big(-e_{15}^{(1)^2}\varepsilon_{11}^{(2)^2} + \gamma_N^{(1)}\mu^{(2)}\varepsilon_{11}^{(1)}\big(\varepsilon_{11}^{(1)^2} + \varepsilon_{11}^{(2)^2}\big)\big),$$
$$V_{11} = -2H_1H_3e_{15}^{(2)}\gamma_N^{(2)}\mu^{(1)}\varepsilon_{11}^{(1)^3}\varepsilon_{11}^{(2)}\big(e_{15}^{(2)}\varepsilon_{11}^{(1)} - 2e_{15}^{(1)}\varepsilon_{11}^{(2)}\big),$$
$$V_{12} = -2H_1H_3\gamma_N^{(2)}\mu^{(2)}\varepsilon_{11}^{(1)^2}\varepsilon_{11}^{(2)^3}\big(e_{15}^{(1)^2} - 2\gamma_N^{(1)}\mu^{(1)}\varepsilon_{11}^{(1)}\big),$$
$$V = V_1 + V_2 + V_3 + V_4 + V_5 + V_6 + V_7 + V_8 + V_9 + V_{10} + V_{11} + V_{12},$$
$$\alpha(s) = R/V, \quad \beta(s) = S/V, \quad \delta(s) = T/V, \quad \gamma(s) = U/V,$$
$$\lim_{s\to\infty}\alpha(s) = \alpha_c, \quad \lim_{s\to\infty}\beta(s) = \beta_c, \quad \lim_{s\to\infty}\delta(s) = \delta_c.$$

Appendix B

$$H_n(\eta, x) = (-1)^{n+1}F_1(\eta, x, n), \quad n = 0, 1, 2, 3, \ldots, \text{ for } 0 < x < l - \eta,$$
$$H_n(\eta, x) = -F_2(\eta, x, n), \quad n = 0, 1, 2, 3, \ldots, \text{ for } x > l + \eta,$$
$$F_1(\eta, x, n) = \frac{\eta^{n+1}}{\sqrt{(l-x)^2 - \eta^2}[(l-x) + \sqrt{(l-x)^2 - \eta^2}]^{n+1}},$$
$$F_2(\eta, x, n) = \frac{\eta^{n+1}}{\sqrt{(x-l)^2 - \eta^2}[(x-l) + \sqrt{(x-l)^2 - \eta^2}]^{n+1}} \quad (\eta = a, b).$$

References

Chen, Z.T., Yu, S.W., 1998. Anti-plane vibration of cracked piezoelectric materials. Mech. Res. Commun. 25, 321–327.

Erdelyi, A., 1954. Tables of Integral Transforms. McGraw-Hill, New York.

Gradshteyn, I.S., Ryzhik, I.M., 1980. Table of Integral, Series and Products. Academic Press, New York.

Huang, H.-M., Shi, H.-J., Yin, Y.-J., 2002. Multi-cracks problem for piezoelectric materials strip subjected to dynamic loading. Mech. Res. Commun. 29, 413–424.

Itou, S., 2001. Stress intensity factors around a crack in a non-homogeneous interface layer between two dissimilar elastic half-planes. Int. J. Fracture 110, 123–135.

Li, X.F., Tang, G.J., 2003. Antiplane interface crack between two bonded dissimilar piezoelectric layers. Eur. J. Mech. A Solids 22, 231–242.

Meguid, S.A., Wang, X.D., 1998. Dynamic antiplane behaviour of interacting cracks in a piezoelectric medium. Int. J. Fracture 91, 391–403.

Narita, F., Shindo, Y., 1998. Dynamic anti-plane shear of a cracked piezoelectric ceramic. Theoret. Appl. Fract. Mech. 29, 169–180.

Narita, F., Shindo, Y., Watanabe, K., 1999. Anti-plane shear crack in a piezoelectric layer bonded to dissimilar half spaces. JSME Int. J. Ser. A 42, 66–72.

Ratwani, M., Gupta, G.D., 1974. Interaction between parallel cracks in layered composites. Int. J. Solids Structures 10, 701–708.

Shindo, Y., Minamida, K., Narita, F., 2002. Antiplane shear wave scattering from two curved interface cracks between a piezoelectric fiber and an elastic matrix. Smart Mater. Struct. 11, 534–540.

Soh, A.K., Fang, D.N., Lee, K.L., 2000. Analysis of a bi-piezoelectric ceramic layer with an interfacial crack subjected to anti-plane shear and in-plane electric loading. Eur. J. Mech. A Solids 19, 961–977.

Takakuda, K., 1982. Scattering of plane harmonic waves by cracks. Trans. Japan Soc. Eng. Ser. A 48, 1014–1020 (in Japanese).

Wang, X.D., Meguid, S.A., 2000. Modelling and analysis of the dynamic behaviour of piezoelectric materials containing interacting cracks. Mech. Mater. 32, 723–737.

Zeng, X., Rajapakse, R.K.N.D., 2000. Crack amplification and shielding in plane piezoelectric solids. Composites: Part B 31, 391–404.

Zhou, Z.G., Han, J.C., Du, S.Y., 1998. Investigation of the scattering of harmonic elastic waves by a finite crack using the non-local theory. Mech. Res. Commun. 25, 519–528.

Zhou, Z.G., Wang, B., 2002. The behavior of two parallel symmetry permeable interface cracks in a piezoelectric layer bonded to two half piezoelectric materials planes. Int. J. Solids Structures 39, 4485–4500.